International Journal of Sustainable Progress
Volume 2, Issue 1, June 2023
http://globalpublisher.org/journals-1001/

Software Modeling of the Effect of Different Topographies of the Zagros Mountain Range in Iran on the Wind Regime to Achieve a Suitable Area for the Construction of Wind Power Plant

Saeid Zamanian [1], Amirsina joorabli [2,*], Davoud Atashbozorg[3]
1- Electrical Engineering, Sahand University of Technology, Tabriz, Iran
saeidzamanian94@gmail.com
2- Energy Systems Engineering Department, Marine Sciences and Technologies Faculty, Islamic Azad University, Tehran, Iran
*Corresponding Author: **Amirsinajoorabli@gmail.com**
3- Energy Systems Engineering Department, Marine Sciences and Technologies Faculty, Islamic Azad University, Tehran, Iran
d.atashbozorg@gmail.com

ABSTRACT

To improve the overall efficiency of a wind power plant, wind regime of the region in terms of wind speed, Wind durability, turbulence of wind regime of the region and k, C_t, C_p variables, will be examined in order to reduce losses for achieving maximum power generation from wind energy. In this research, mountainous Areas of north western of Iran which has a appropriate wind regime for constructing of the power plant in terms of wind regime variables and regional components for wind power plant construction, is being examined.In this study, 6 regions with different topographies and completely different altitudes have been selected. These points have been modeled and analyzed by using the specialized wind analysis software (wida) and finally by using the diagrams obtained from the software with specialized analysis of the charts according to the effective parameters in locating the wind turbine installation site for producing maximum energy and minimizing the risks caused by passible attacks of the regional wind regime. First, the region is examined in terms of the wind regime formed in the region based on the prevailing topography in the region, finally the areas has been investigated for wind energy attacks for friction and early failure of wind turbines. Comparing downscaled numerical weather prediction wind speed with measurements from a large number of stations throughout Iran resulted in overall improved correlations and distribution statistics. Since we used a large number of model topographies to derive the subgrid parameterization and the downscaling framework, 6 regions are not scale dependent nor bound to a specific geographic region. 6 regions can readily be implemented since they are based on easy to derive terrain parameters. Finally by comparing the results obtained from the software for these 6 regions, the direct effect

of the height of the region on the wind speed on the ground and at a Height of, 100 meters, direct impact of topography and wind roughness on wind formation and wind speed of the region, identify the prevailing wind direction in 6 areas. Direct impact of topography on the ratio of vertical speed changes in the region and finally the effect of the variables k, c, at modeled velocities, is obtained.

Keywords: wind energy, computational fluid dynamics, wind regime modeling, earth topography, multiverse optimization, Weibull distribution, wind resource assessment, numerical methods, wind data

1. INTRODUCTION

Today, the use of renewable energy sources is growing day by day, and the use of wind energy and wind farms has the largest share in this growth. Although the use of these energy resources has been economical, to get the most out of this energy, the topological features of the extraction site play an important role. One of the most important goals of this research is to achieve the best point for the construction of wind turbines to achieve maximum turbine production capacity in mountainous areas with high turbulence. The most important effect of this research is on the process of site identification and better understanding of wind resources analysis. This process will ultimately play a significant role in the micro-siting and more accurate design of the wind farm and increase the efficiency of these power plants.

Complex topography is known to influence the surface energy balance in mountainous terrain. This is in part caused by the wind field controlling turbulent heat and vapor exchange. Boundary layer wind fields are significantly altered by topography, giving rise to sheltering in lee directions or speed up in windward directions of mountain slopes.

Estimating wind conditions in areas with complex natural features and considering that input information should be considered for a large area, basically requires simulation and modeling calculations. Just as obstacles can cause turbulent flows, the presence of hills, mountains, and the complexity of topography or forest and precipice can also cause turbulent flows, so the more complex the topographic conditions, the more turbulent currents are formed. In this research, the study area (different mountainous areas of the northwestern strip of Iran) that has different topographies will be considered. The purpose of selecting this area is to investigate the effect of mountaineering features with different angles and shapes on wind speed and the effect of these slopes will be done by modeling the software and reviewing and analyzing the graphs. Finally, the results are compared with each other and the effects of different topographies on the wind regime are examined and concluded. Mountaineering or large vertical effects on the earth's surface can have a major effect on wind speed profile. In real life, wind currents are not only exposed to the effects of hills, ridges and precipices, but the effects of these effects are very significant. It is important to know how the wind blows on a hill to affect the environment. This study analyzes these effects and their effects on wind flow.

2. LITERATURE REVIEW

Complex topography is known to influence the surface energy balance in mountainous terrain [21]. This is in part caused by the wind field controlling turbulent heat and vapor exchange. Boundary layer wind fields are significantly altered by topography, giving rise to sheltering in lee directions or speed up in windward directions of mountain slopes.

Topography is mostly unresolved in course-scale atmospheric models, especially over alpine terrain. This leads to underestimated topographic impacts on predicted variables [18,14,5]. Unresolved topographic features are however relevant for surface wind field simulations [1,20,16]. Complex topographic features lead to a net drag of turbulent flow associated with a phase shift of the pressure field relative to the topographic features [26]. Because of this net drag, area-averaged wind speed over topography are lower. Accounting for the effects of unresolved fine-scale orography on wind speed in coarse grid cells is therefore required.

Parameterizations for gravity wave drag and flow blocking due to meso-scale mountain ranges are commonly applied in numerical weather prediction (NWP) models [17]. With the increased horizontal grid cell resolutions in climate or NWP models, turbulent form drag (drag below the blocked flow drag) exerted by subgrid topography also needs to be accounted for. Turbulent form drag thus acts on scales smaller than the gravity wave and flow-blocking dynamics. Unresolved drag was originally tackled by introducing an effective roughness length to describe the momentum loss to the surface over mountainous terrain [6, 19]. Applying this so-called effective roughness length approach increases the surface roughness length based on the underlying topography. Area-averaged wind profiles, using the effective roughness length, are assumed to follow a logarithmic height profile similar to the wind profile using a surface roughness length [25,26]. Turbulence data measured well above topography confirmed the effective roughness length concept [8].

Given these studies, it was concluded that an effective roughness length can be applied to parameterize the drag in NWP models [26, 1, 4]. However, some important limitations exist such as corrections for overestimations in heat- and moisture-related processes [27, 1, 16]. A different approach therefore introduced turbulent form drag as an extra sink term (momentum flux) in the momentum equations [27]. The overall form drag induced by subgrid topography on mean wind speed is then treated using a concept similar to existing gravity wave drag parameterizations in meteorological models.

Nowadays, many NWP models have implemented the concept of Wood et al. [2001]. Various terrain parameters are used to scale subgrid topographic drag on mean wind speed, virtually all related to slope parameters. Jimenez and Dudhia [2012] suggested a combination of the standard deviation of subgrid terrain elevations and a nondimensional version of the Laplacian of resolved terrain elevations using empirical thresholds. Beljaars et al. [2004] also suggested a formulation applying the standard deviation of subgrid terrain elevations. Rontu [2006] proposed a simplified version of the parameterization of Wood et al. [2001] to describe orographic drag due to unresolved fine-scale topography in the High-Resolution Limited Area Model (HIRLAM) based on the mean maximumof subgrid slopes in a coarse grid cell.

Suggested terrain parameters to parameterize unresolved form drag were only empirically derived. Mostly numerical model experiments were used for verification with a previous model version as reference. Furthermore, a limited number of ground stations in specific geographical regions were used for validation of coarse-scale wind speed. For instance, Rontu [2006] used Icelandic synoptic stations whereas Jimenez and Dudhia [2012] used measured ground wind speed in the northeast of the Iberian Peninsula. It is however questionable if coarse-scale simulated wind speed can represent measured wind speed at the ground in complex topography. Wind speeds can show large spatial variability below typical NWP model grid cell sizes. Without using terrain parameters but also covering hilly areas Sweeney et al. [2013] found reduced wind speed errors when applying adaptive statistical postprocessing methods on NWP output. This approach required training each day on data from previous days and was also only tested for stations around Ireland.

3. METHOD

In this study, 6 areas with different topographies were selected and modeled and analyzed using specialized software for a height of 100 m above the ground, and the variables of the wind regime for each were obtained separately. In the first stage, the regions are analyzed by topography, in the second stage, the regions are examined in terms of wind regime variables.

Instead of simulating spatial wind speed fields on a limited number of real topographies, which can bias our conclusions, we simulated wind fields on isotropic Gaussian random fields (GRF) with a Gaussian covariance as a simplified topography model. Gaussian statistics give a reasonable description of various geometrical characteristics of real, complex topographies. For a set of real topographies from the U.S. and Switzerland, averaged standard deviations of slope components in orthogonal directions were roughly isotropic which further motivated the constraint to isotropic GRF as model topographies. Furthermore, stochastic topographies were successfully applied to analyze radiative transfer in complex topography and to generalize an analytical approximation of the sky view factor in complex terrain for coarse grid cells. Since simulated topographies from discretized GRF can cover a wide variety of topographic characteristics, they allowed us to conduct a detailed analysis of domain-averaged (i.e., average over a grid square) simulated wind speed in complex terrain. And finally, the regions are compared and statistically analyzed.

4. CASE STUDY AREA

In this study, 6 areas with completely different topographies and heights from different land levels are examined. Table 1 shows the area specifications.

Table 1. Specifications of the studied areas

Num	Type of topography of the area	Above sea level (m)	Coordinates	
			Long	Lat
1	Valley - Flat	2200	44.5637	38.492046
2	Valley - Flat (residential area)	2100	44.4762	38.080796
3	Flat (residential area)	2000	44.3937	37.933006
4	Mountaintop	2300	44.7001	36.734381
5	Mountainous (Complex topography)	1000	44.722	36.632371
6	Rolling Road	900	44.1918	36.255362

4.1. Smooth Valley [7]

In this section, we consider a single valley with a medium depth for Region 1. The formation of a forced canal creates a current of wind flowing along the axis of the valley, and a sudden reversal of the direction of the wind when the flow of air flows from a line perpendicular to the axis of the current valley. The turbulent downward displacement of the horizontal momentum, which also occurs on flat ground, creates wind directions in the valley that are similar to the direction of the wind flow with slight rotation due to friction near the ground. During the formation of the canal, the winds inside the valley are created by the gradient component of the wind flow pressure along the valley axis, and the return of the wind direction occurs when the wind moves along the valley axis. The relative importance of different streams depends on the size, depth and width of the valley.

4.2. Smooth Region

The simplest type of land is regional, which can be described as smooth and almost homogeneous by considering the surface characteristics of the stream that affects the boundary layer. The type of soil in these areas is usually clay. Soil is sandy and so on. In this position, horizontal air movement can be avoided and the system can be considered in local equilibrium conditions. According to the similarity theory, the vertical structure of the Earth's atmospheric boundary layer, and of these two vertical profiles, the aerometric variables are determined by the disturbed surface fluids of the momentum, temperature and humidity. The wind flow characteristics (wind speed and direction) are then determined by the current (or larger scale) flow source, which is outside the vertical structure of the dominant atmospheric boundary layer, with changes determined by local surface fluids with It fits.

4.3. Hill land

We can define a hilly terrain as a topography made by rows of hills and valleys, or more generally, the alignment of individual hills. Atmospheric flow at the top of a medium-sized hill is a case of wind flow in a complex topographic zone, which has undergone many theoretical and experimental studies over the past 20 years. Experimental studies have been performed in the atmosphere and laboratories. Changes in disturbed values were investigated in depth. These

studies made it possible to obtain a satisfactory knowledge of the changes created by a single topographic barrier in moderate and turbulent atmospheric variables under neutral and constant conditions.

The main characteristics of the flow at the top of a hill are determined not only by the shape of the hill but also by its size and atmospheric stability. In steady-state conditions, vertical displacement of air occurs when the wind is blowing along the hill, in the opposite direction to the gravitational force, and then the current is affected by the bionic force. If the size of the hill is large enough to change the entire depth of the boundary layer, the boundary effects can also be significant during the day due to the thermal layering at the top of the atmospheric boundary layer. In neutral conditions, the current generally indicates a decrease in velocity near the foot of the hill windbreak and acceleration on a slope in the opposite direction to the wind. The maximum speed is near the top of the hill. A significant decrease in current on the back side of the hill has been observed, which can cause the separation of the flow and the very turbulent area. The presence of a constant vertical temperature gradient affects the intensity and position of topographic disturbances. In stable conditions, the kinetic energy of the flow may not be sufficient to raise the air above the hill. Wind flow is more likely to flow around a hill than it is to flow over the hill, in which case the concept of dividing line can be introduced. The dividing line separates the vertical lines that pass through the top of the hill from the ones around it vertically.

Even a short hill creates significant disturbances in the flow that can have a detrimental effect on dispersion. In neutral or low conditions, the flow at the top of a hill can be completed by analytical solutions of Navier Stokes equations based on linearization methods as a low-cost alternative to numerical solutions of a complete set of equations. Survival is described. The topographic flow discussed in this section can generally consider the characteristics of the local scale flow.

4.4. Complex topography

Complex topography can be summarized as landscaping, commonly known as mountains. This type of land is made up of systems of barriers and valleys, which can be identified by steep slopes, increasing thermal circuits such as mountain-valley breezes, the wave it creates mountain streams and drastically changes the flow characteristics.

Mountain-valley breezes are more easily seen in tornadoes in summer. In such situations, a slight warming around the mountain of horizontal gradations increases the temperature and pressure that the winds create. The characteristics of wind systems depend on the geometry and orientation of the valley. Mountain winds can generally be divided into two categories: down winds and valley winds.

Falling winds are created by the bovine forces by the temperature difference between the air adjacent to the inflow and the ambient air at the same height away from the inflow (e.g. in the center of the valley). Low winds blow upwards during the day and downwards during the night. To maintain continuity, a closed circulation is developed throughout the valley, which includes the downward moving air in the center of the valley during the day and upwards during the night. The circulation of the valley transfers heat by heating or cooling the entire valley space

throughout the valley and thus contributes to the development of valley winds. These winds are created by horizontal compressive gradients that develop as a result of the temperature difference between the air inside the valley and the air at the same height on the adjacent plate. The valleys wind parallel to the longitudinal axis of the valley in the upward direction of the valley during the day and the bottom of the valley during the night. This circulation is closed at the top of the mountain ridges by the reverse flow of the wind in the opposite direction. The actual development of thermally generated winds is often complicated by other wind systems developed on a variety of scales. These thermal winds show significant seasonal changes in frequency and intensity that are generally stronger during the summer, while snow-covered slopes during the winter can create cold breezes that can occur during the summer. The day will remain [12].

5. SIMULATED WIND FIELDS

We computed high-resolution atmospheric wind flow fields with the three-dimensional nonhydrostatic and compressible atmospheric model Advanced Regional Prediction System (ARPS), developed at the Center for Analysis and Prediction of Storms (CAPS), University of Oklahoma. Simulated ARPS wind fields, replicated typical measured wind field characteristics well, even over real complex topographies. Using ARPS wind fields, even snow drift in very complex terrain was successfully modeled. ARPS is therefore suitable to investigate spatial wind speed over complex terrain.

Since the focus in this study was to analyze the influence of topography on wind speed, we suppressed thermally induced circulations like mountain valley breezes by neglecting radiation effects and by setting atmospheric stability to neutral, i.e., the sub grid parameterization and the downscaling scheme are developed for neutral atmospheric stability. This was done for two reasons. First, our main focus is on the drag exerted by topography on near-surface wind flow, which was found under neutral static conditions. Second, to account for a variety of atmospheric stabilities, especially over snow-covered terrain, a large number of additional ARPS simulations would be required. This is beyond the scope of our work, for which we already performed ARPS simulations on a total of 9000 model topographies. Furthermore, Cullen et al. [2007] showed that near-neutral conditions dominate over snow-covered complex terrain.

5.1. Modeling using specialized software [15]

This software is useful in the field of turbines and wind farms, which uses a linear method to analyze wind energy equations and wind data. The procedure with this software is as follows:

5.2. Principles of energy calculation

General information for energy calculations has two main sets of data needed to estimate AEP for a turbine: the distribution of wind speed at the height of the turbine hub and the power curve for the turbine corrects the air density and ultimately corrects the turbulence. If more turbines are to be placed side by side and in clusters or a wind farm, the wind speed distribution, the exact location of the turbines, and the C-curve must also be known.

5.3. Wind speed distribution

The distribution of wind speed indicates the probability of a certain wind speed versus wind speed. The two parameters of the probability distribution of the weibull are often used to express the wind speed distribution. Figure 1 shows examples of a wobble measurement distribution curve.

5.3.1. Distribution Characteristics for Wind Data

The dynamic nature of wind can be studied with the application of the probability density function. The probability density function f (v) gives an idea about the occurrence of wind velocity and the cumulative distribution F(v) tells whether the wind velocity is less than or equal to that wind velocity. There are several methods that can be applied to analyze the wind data for estimating the wind potential [13,14] for a particular region. It was found from the literature that Weibull and Rayleigh [15] are the most preferred methods for determining the wind energy potential. In order to implement the Weibull and Rayleigh distribution, we need to estimate the shape and scale parameter. Many researchers have done studies for evaluating the wind potential through different probability density function. The results showed that the Weibull and Rayleigh distribution have presented the wind distribution in a better manner [16–24].

5.3.1.1. Weibull Distribution

This distribution has been used for many years for fitting source data, i.e., actual wind data. The wind data characteristics in any region can be analyzed by using the probability distribution function [25,26].

Another approach is to follow the Rayleigh distribution, which has also been used as one of the statistical tools to analyze wind data. To perform both Weibull and Rayleigh we required shape and scale parameters (k and c) [27]. The shape parameter value decides the type of distribution whether it should be Weibull or Rayleigh. When the shape parameter is less than 2 then it takes a Weibull distribution. When it is exactly 2 it is known as the Rayleigh distribution, if it exceeds 3 it takes the Gaussian distribution [28].

The Weibull distribution function or Weibull probability density function is calculated as [29]:

$$f(v) = \left(\frac{k}{c}\right)\left(\frac{v}{c}\right)^{k-1} e^{-\left(\frac{v}{c}\right)^{k}} \quad \textbf{(1)}$$

Where, f (v) is the probability of wind speed, v is the wind velocity, k and c are the shape and scale parameters. k has no dimensional units whereas the c parameter has the dimensional unit as (m/s), similar to wind speed.

On integrating the Weibull probability distribution, we get the Weibull cumulative distribution function [30] and it is expressed as:

$$F(v) = \int_0^a f(v)dv = 1 - e^{-(\frac{v}{c})^k} \quad \textbf{(2)}$$

where α represents the highest wind speed under consideration and it changes according to the site.

The expected value of the wind speed otherwise known as the average wind velocity is obtained from the Weibull distribution parameters of k and c and is given by:

$$v_m = c\Gamma\left(1 + \frac{1}{k}\right) \quad \textbf{(3)}$$

where "Γ" is known as the gamma function and it is defined as:

$$\Gamma(t) = \int_0^\infty x^{t-1}e^{-x}dx \quad \textbf{(4)}$$

Now the standard deviation for the Weibull distribution is given as:

$$\sigma = c\sqrt{\Gamma\left(1 + \frac{2}{k}\right) - \Gamma^2\left(1 + \frac{1}{k}\right)} \quad \textbf{(5)}$$

After calculating the values of σ and υ_m , the shape and scale parameters can be evaluated as follows:

$$\left(\frac{\sigma}{v_m}\right)^2 = \frac{\Gamma\left(1 + \frac{2}{k}\right)}{\Gamma^2\left(1 + \frac{1}{k}\right)} - 1 \quad \textbf{(6)}$$

From expression (6) k can be found and once k is calculated, c is determined from the following:

$$c = \frac{v_m}{\Gamma\left(1 + \frac{1}{k}\right)} \quad \textbf{(7)}$$

Now the Weibull probability density function is found using Equation (1).

5.3.1.2. Rayleigh Distribution

It has already been mentioned that when shape factor "k" is 2 then such a distribution is known as the Rayleigh distribution [30]. Now after rearranging Equation (1), the Rayleigh probability density function is given by:

$$f(v) = \left(\frac{v}{a^2}\right) e^{-\frac{v^2}{2a^2}} \quad \textbf{(8)}$$

where α is the scale parameter and its units are m/s and its value is given by:

$$\alpha = \sqrt{\frac{2}{\pi}} v_m \quad \textbf{(9)}$$

The Rayleigh cumulative distribution F(υ) is calculated from the expression:

$$F(v) = 1 - e^{-\left(\frac{v^2}{2a^2}\right)} \quad \textbf{(10)}$$

In order to calculate the most probable wind speed (V_{MP}) and the most energy (V_{MaxE}) from the wind speed, it can be estimated from the equations as shown below:

$$V_{MP} = c\left(\frac{(k-1)}{k}\right)^{k-1} \quad \textbf{(11)}$$

$$V_{MaxE} = c\left(\frac{k+2}{k}\right)^{\frac{1}{k}} \quad \textbf{(12)}$$

5.4. Performance Measures

We compared subgrid parameterized and downscaled wind speed to ARPS wind fields and to AWS data throughout Iran. To characterize the performances we used a variety of measures: absolute error measures, namely, the root-mean-square error (RMSE), normalized root-mean-square error (NRMSE) (normalized by the range of data), mean- absolute error (MAE), a relative error measure, namely, the bias error (Bias), and the Pearson correlation coefficient r as a measure for correlation. Finally, we judged the performance by analyzing the probability density functions (pdf). We used the two-sample Kolmogorov-Smirnov test (K-S test) statistic values D for the pdf's (nonparametric method), and we computed the RMSE for Quantile-Quantile plots (RMSE quant) for probabilities with values in [0.1, 0.9].

6. RESULTS AND DISCUSSION

In this study, the main concern is associated with topographical effects. The presence of hills, ridges and escarpments can have significant number of effects in different scales of topographic factor. Hills differ from ridges in that the wind can diverge over sides in addition to speeding up over crests. The degree of topographic effects for hill is thus generally less than that for a ridge of the identical slope.

In the considered geophysical features of case studies it is found that types of slope for all case studies are mostly shallow. For shallow topography, no separation of flow occurs. The topographic factor is shown different results by the influence of different parameter in each code and slope of topography in direction wind is blowing. In the comparison of topographic factors, it is found that topographic factor value using the original codes are tended most likely to be greater than that using MPM. The rationalized formula among the codes also has been highlighted to comprehend why the results of topographic factor in each code are different when the wind comes from the identical direction. Hence, it is found that topographic factors are influenced by hill shape factor, distance of structure factor, and height of building factor.

The software output is shown as a graph for wind regime variables, wind direction, wind speed, weibull, and variables C_p, C_t , and k.

- **Region 1**: It has a smooth topography and is located in the valley of a mountainous region with an altitude of 2200 meters above sea level. The diagrams in this area are shown below.

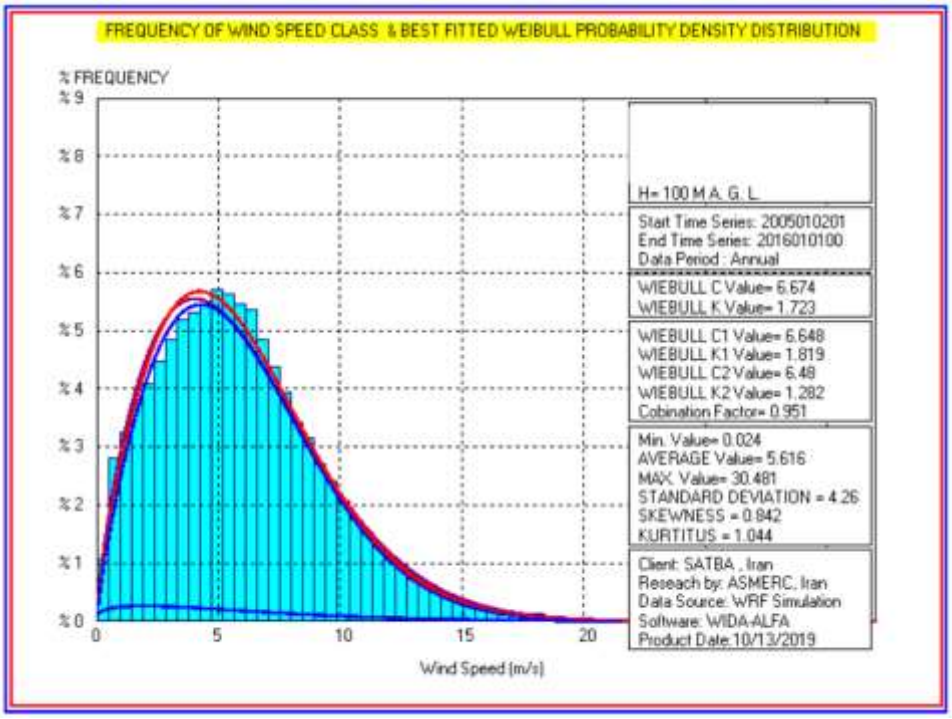

Fig. 1 - Weibull diagram (Region 1)

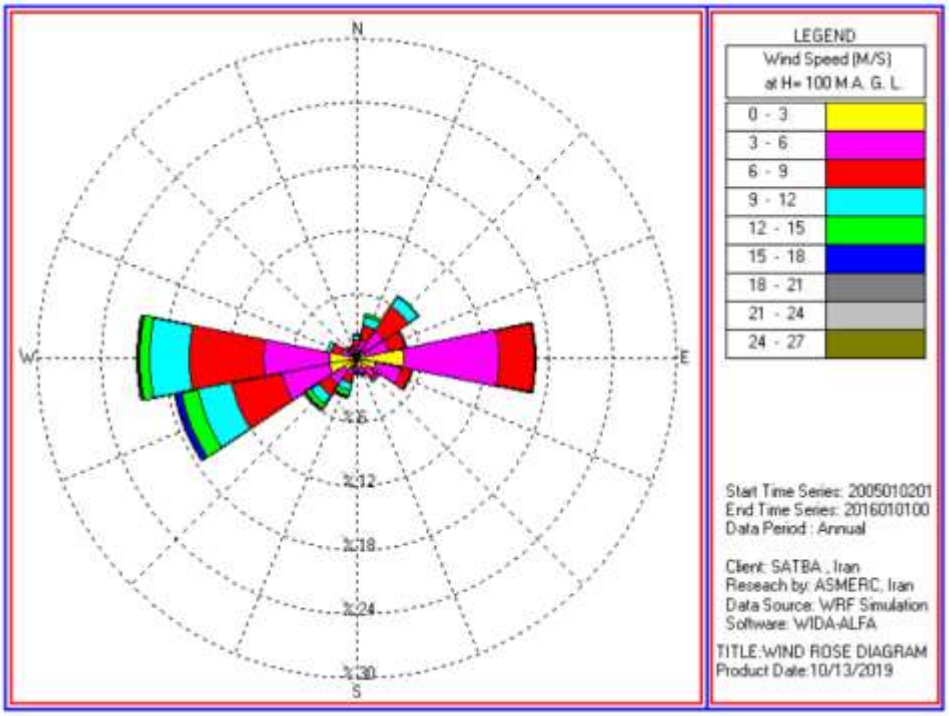

Fig. 2 - Dominant wind direction (Region 1)

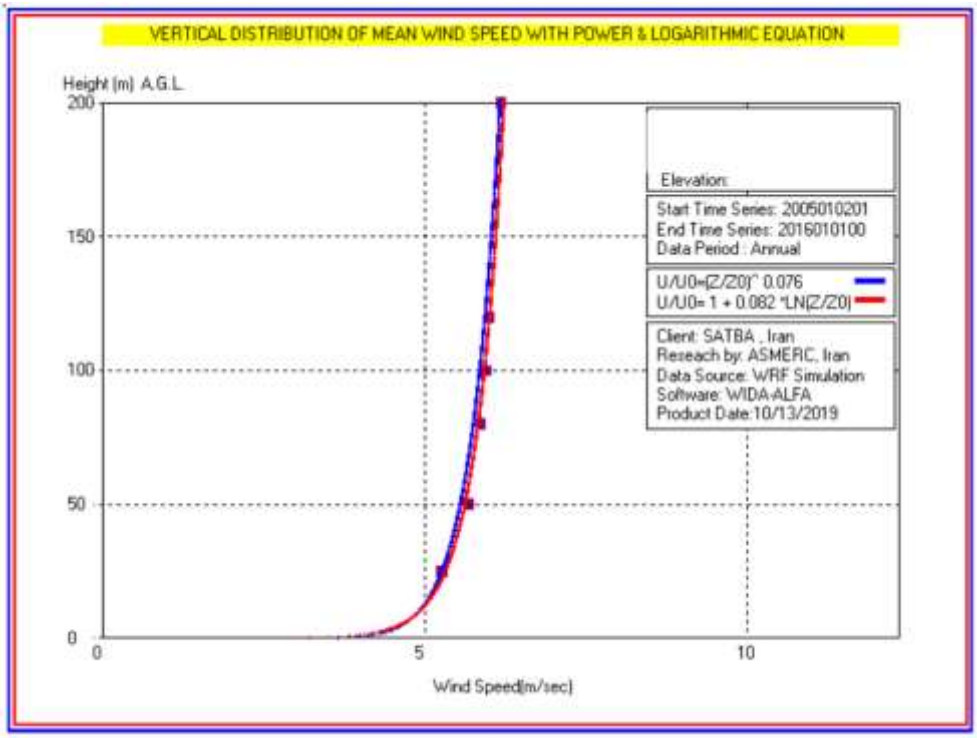

Fig. 3 - Vertical distribution of wind speed with logarithmic equation (Region 1)

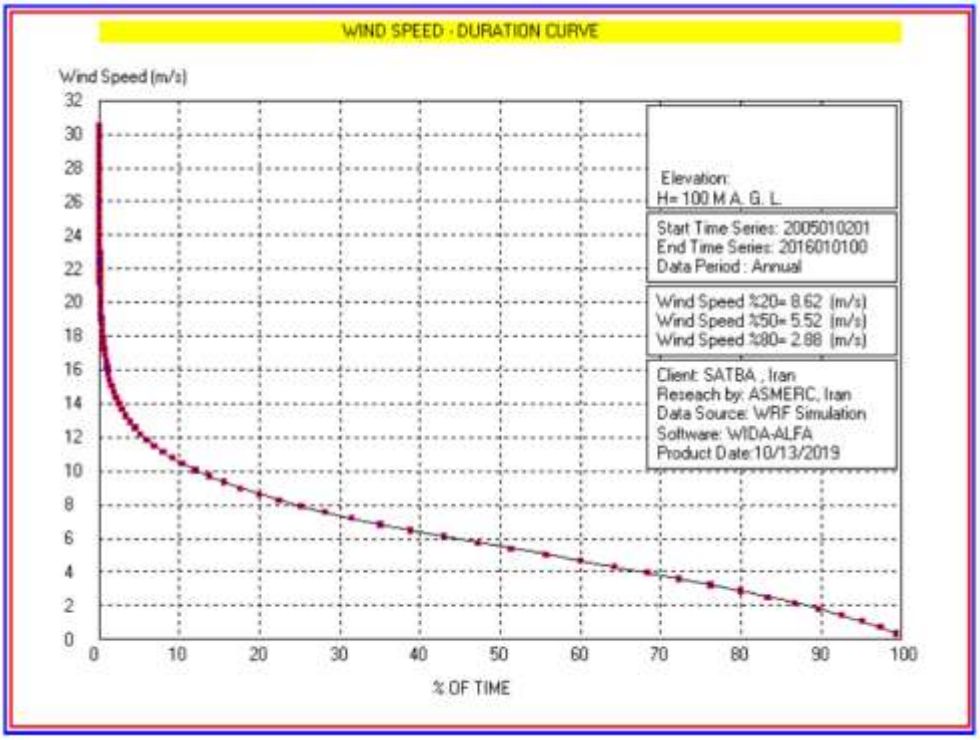

Fig. 4 - Vertical wind speed curve (Region 1)

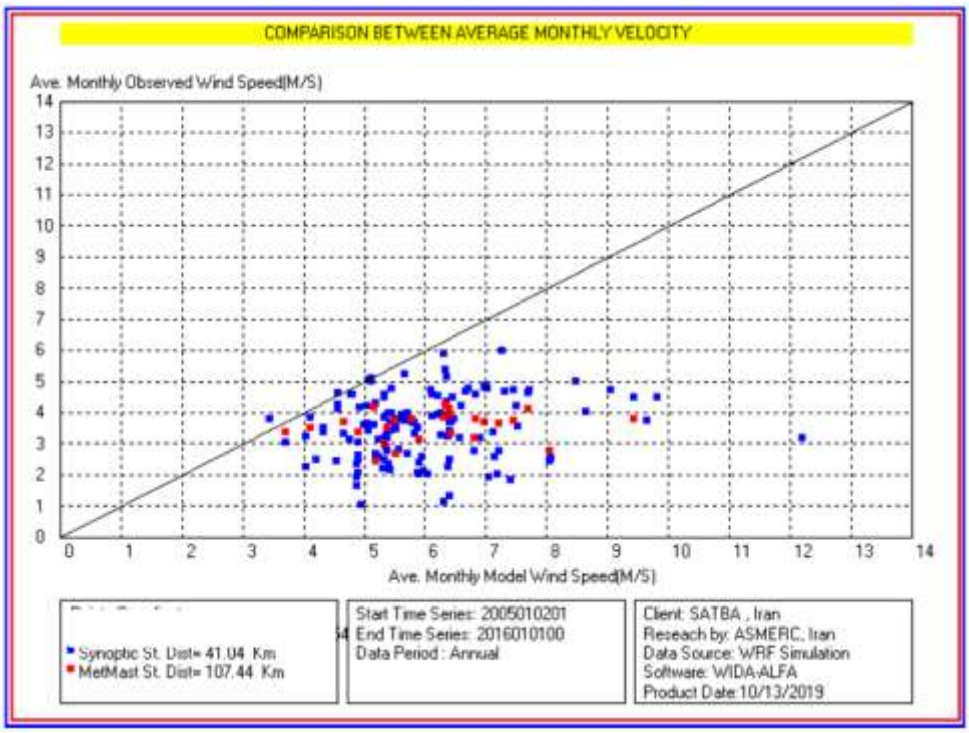

Fig. 5 - Comparison of observed speed with modeled velocity (Region 1)

- **Region 2**: It has a flat topography in the valley and in a residential area, with an altitude of 2100 meters above sea level. The diagrams in this area are shown below.

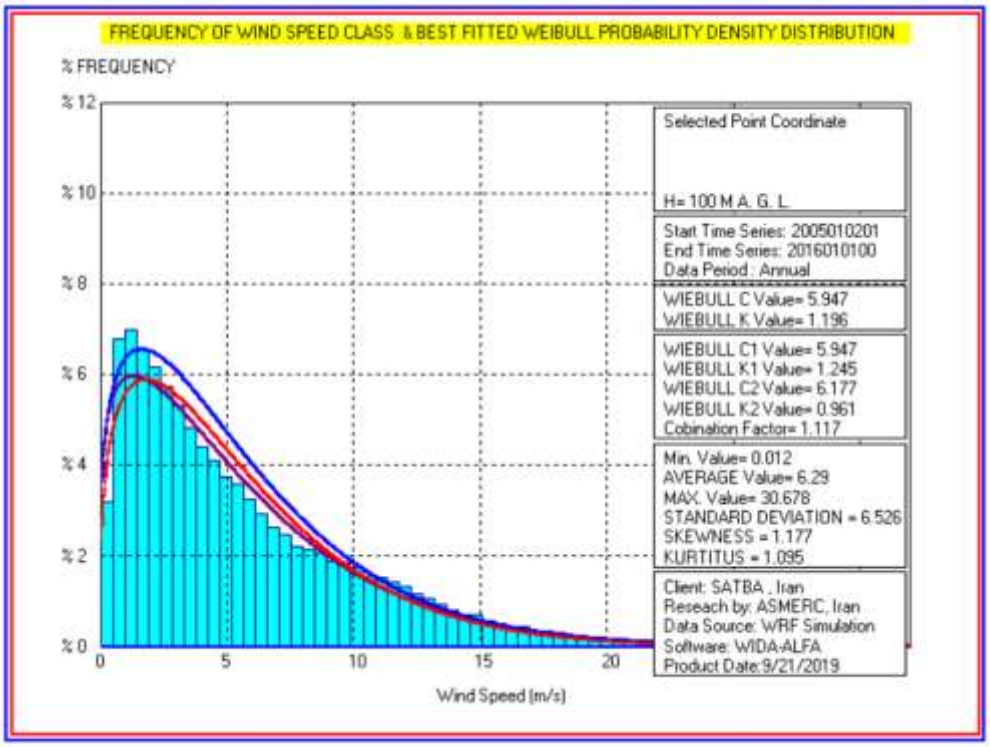

Fig. 6 - Weibull diagram (Region 2)

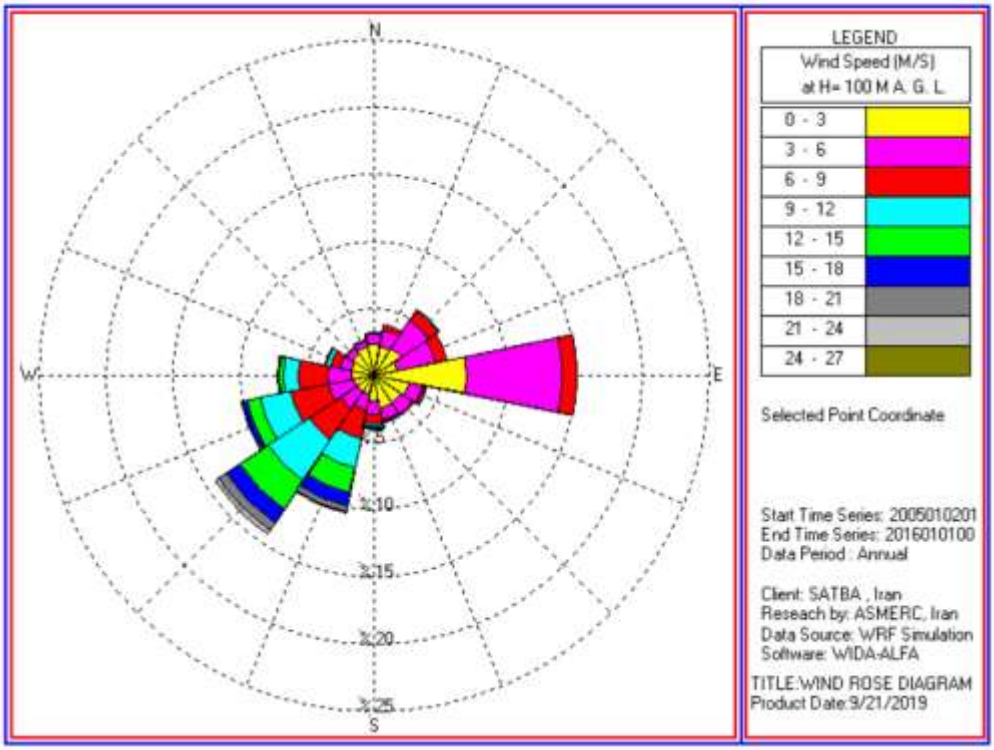

Fig. 7 - Dominant wind direction (Region 2)

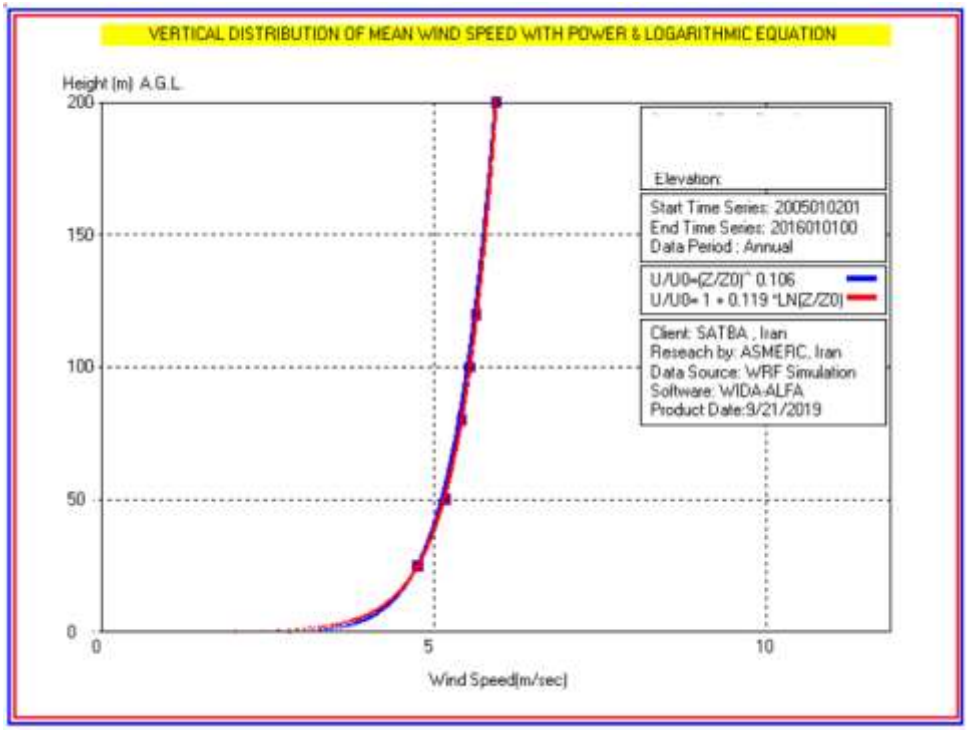

Fig. 8 - Vertical distribution of wind speed with logarithmic equation (Region 2)

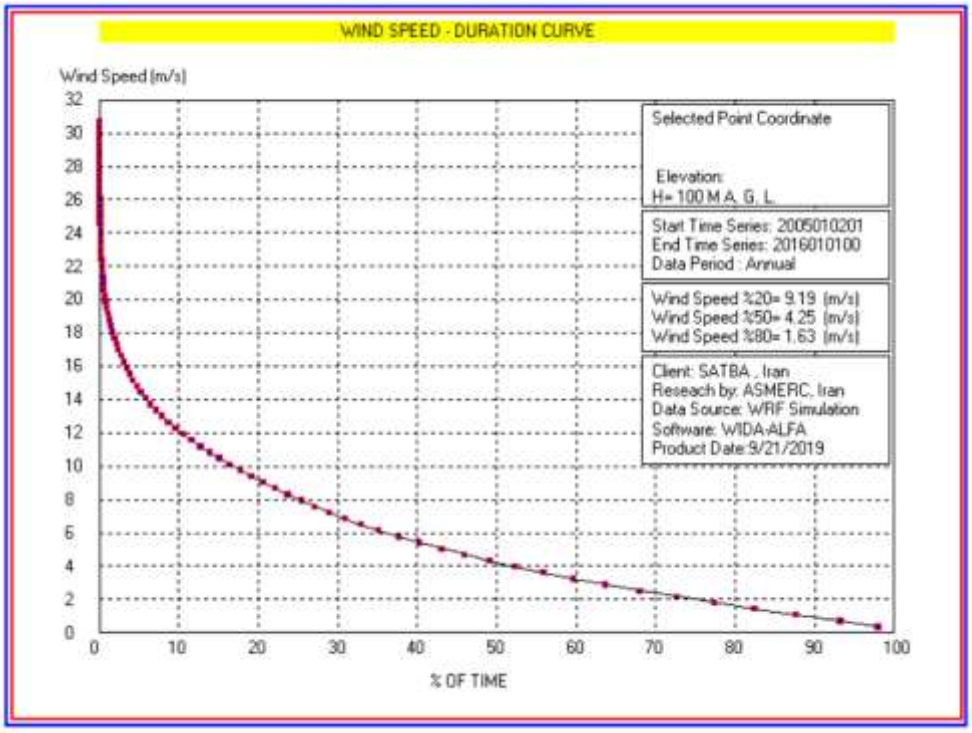

Fig. 9 - Vertical wind speed curve (Region 2)

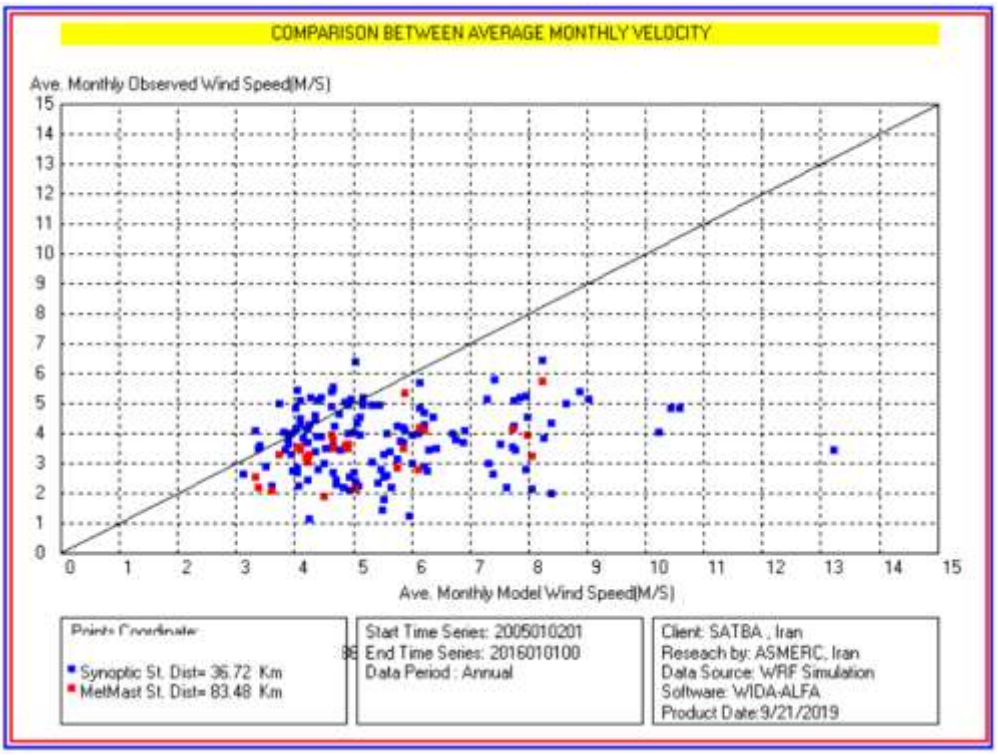

Fig. 10 - Comparison of observed speed with modeled velocity (Region 2)

- **Region 3**: It has a flat topography in a residential area, 2000 meters above sea level. The diagrams in this area are shown below.

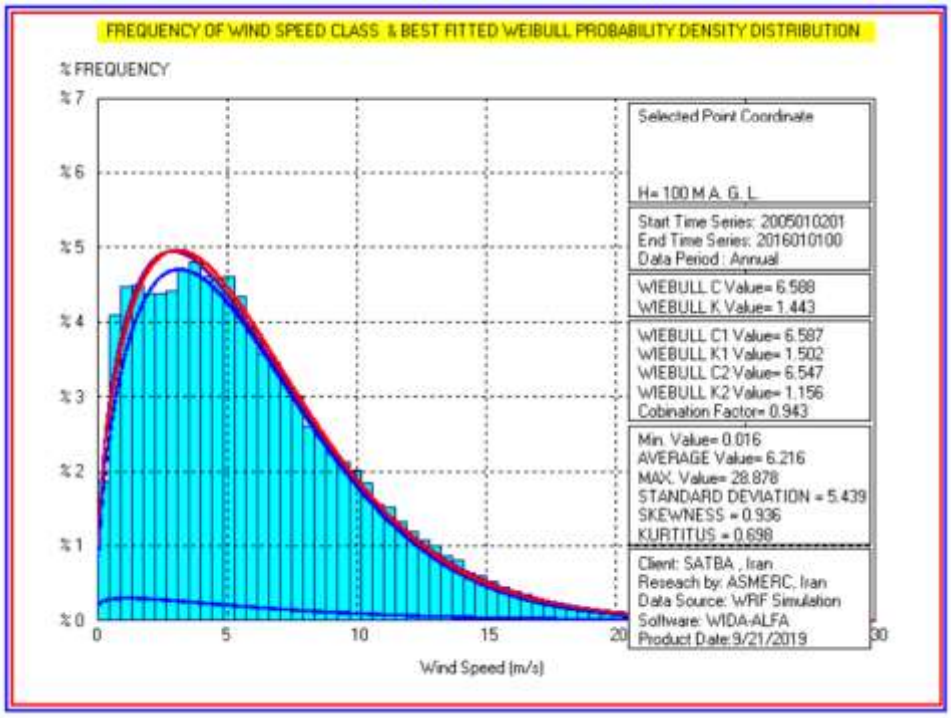

Fig. 11 - Weibull diagram (Region 3)

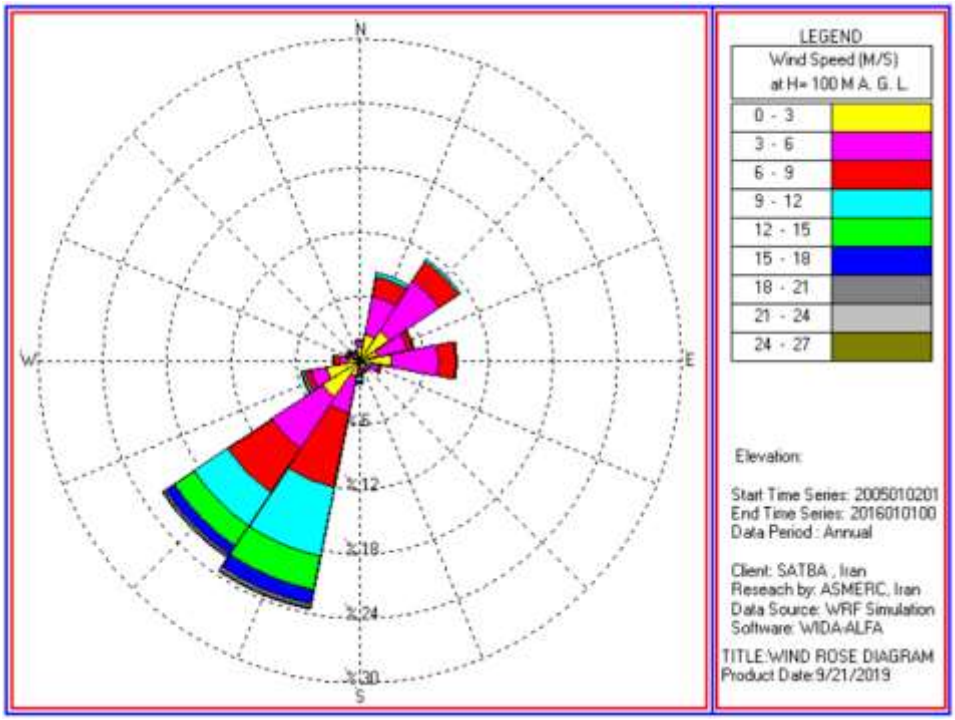

Fig. 12 - Dominant wind direction (Region 3)

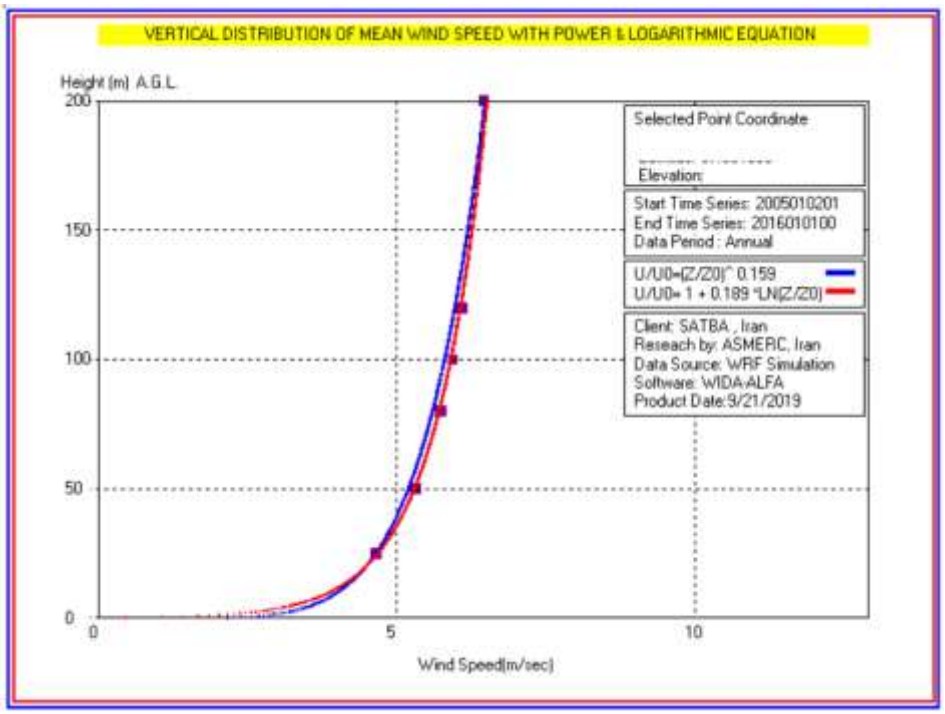

Fig. 13 - Vertical distribution of wind speed with logarithmic equation (Region 3)

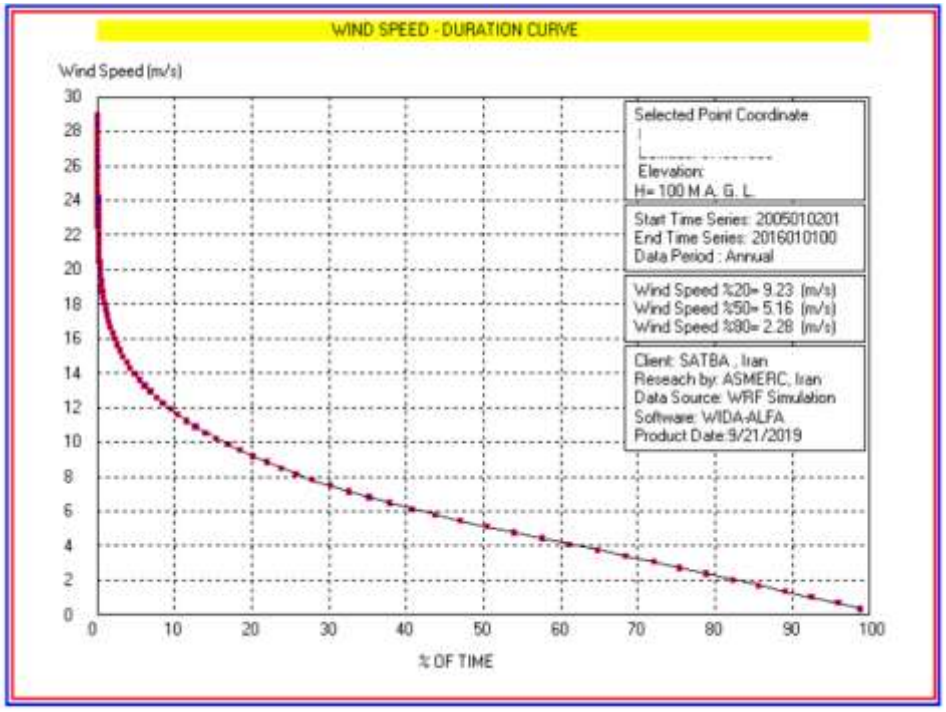

Fig. 14 - Vertical wind speed curve (Region 3)

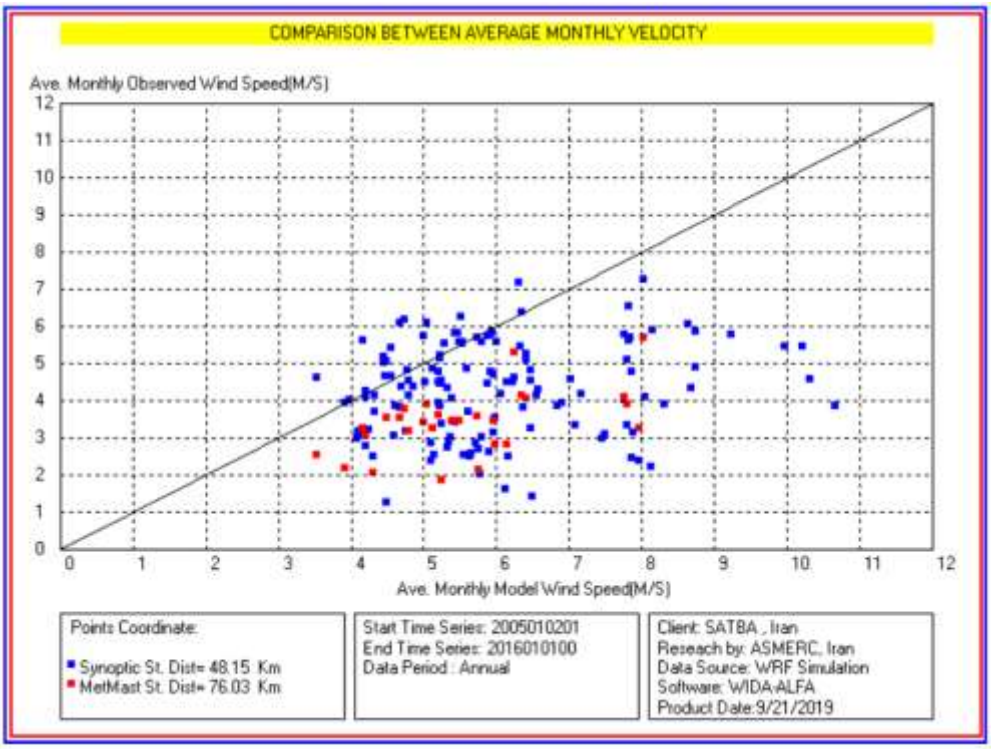

Fig. 15 - Comparison of observed speed with modeled velocity (Region 3)

- **Area 4:** Located on the top of a mountain, 2300 meters above sea level. The diagrams in this area are shown below.

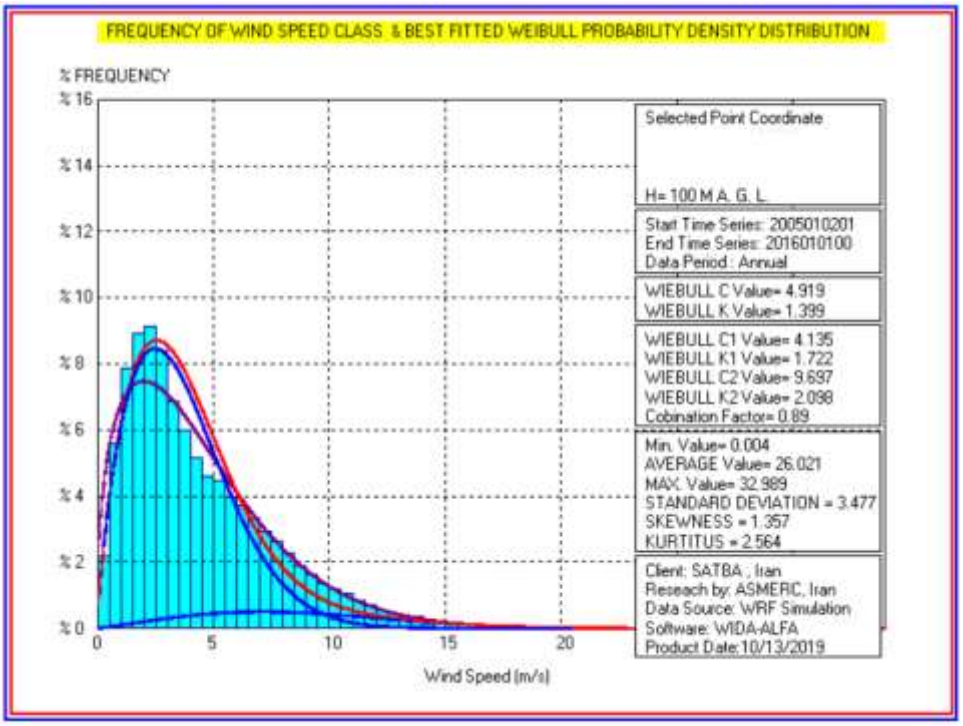

Fig. 16 - Weibull diagram (Region 4)

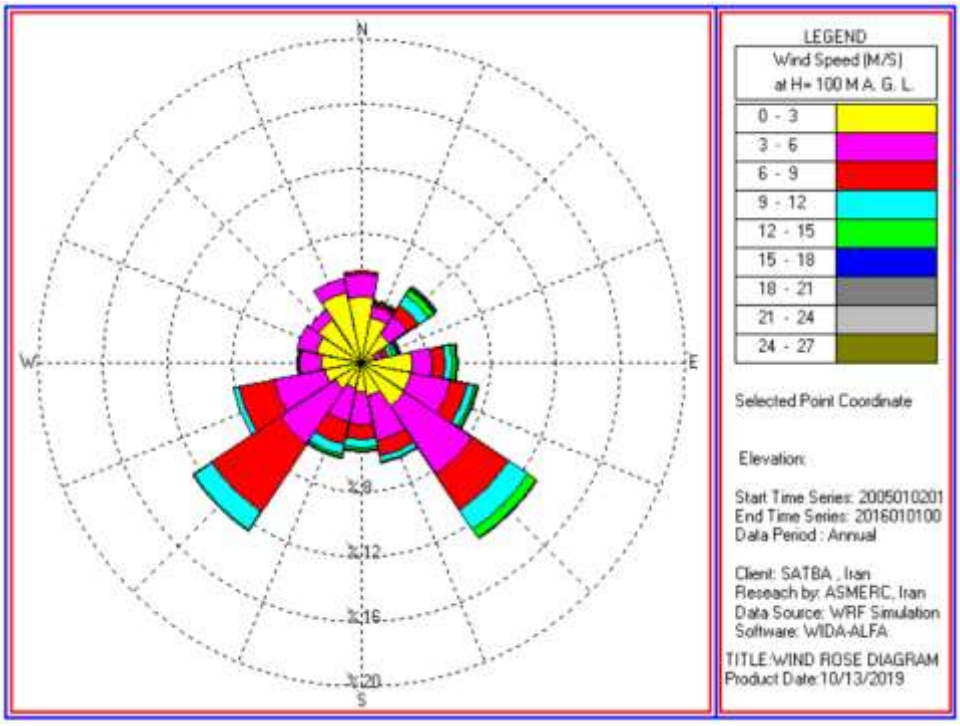

Fig. 17 - Dominant wind direction (Region 4)

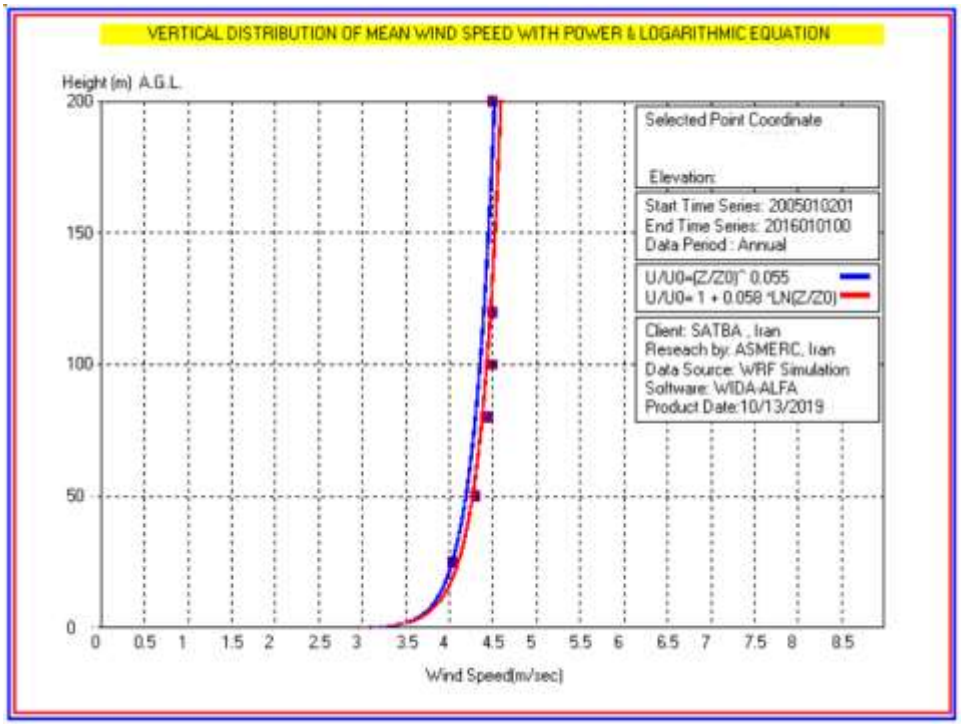

Fig. 18 - Vertical distribution of wind speed with logarithmic equation (Region 4)

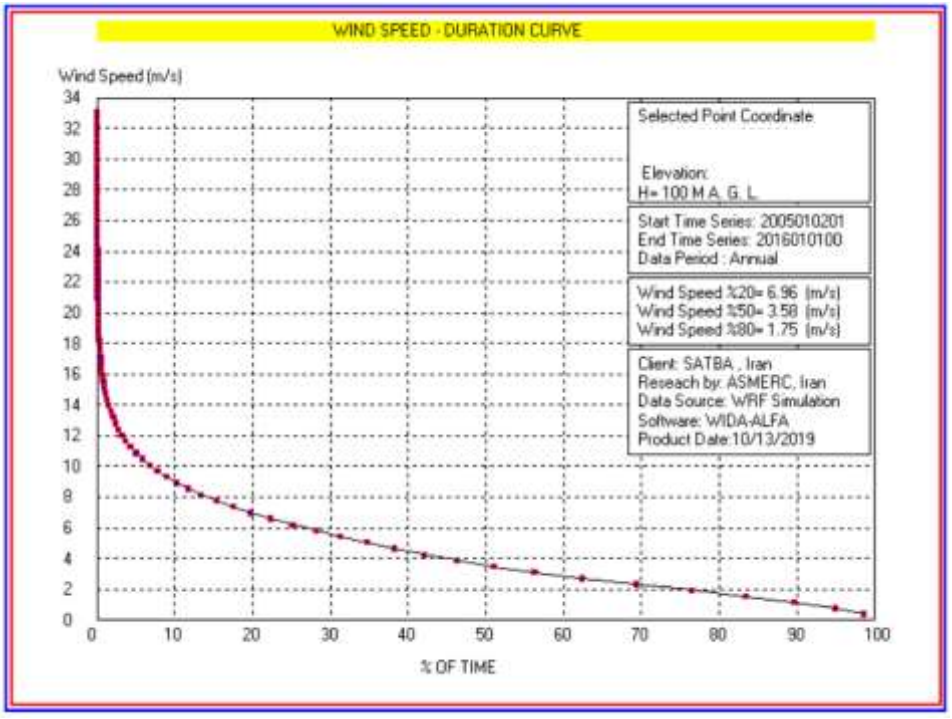

Fig. 19 - Vertical wind speed curve (Region 4)

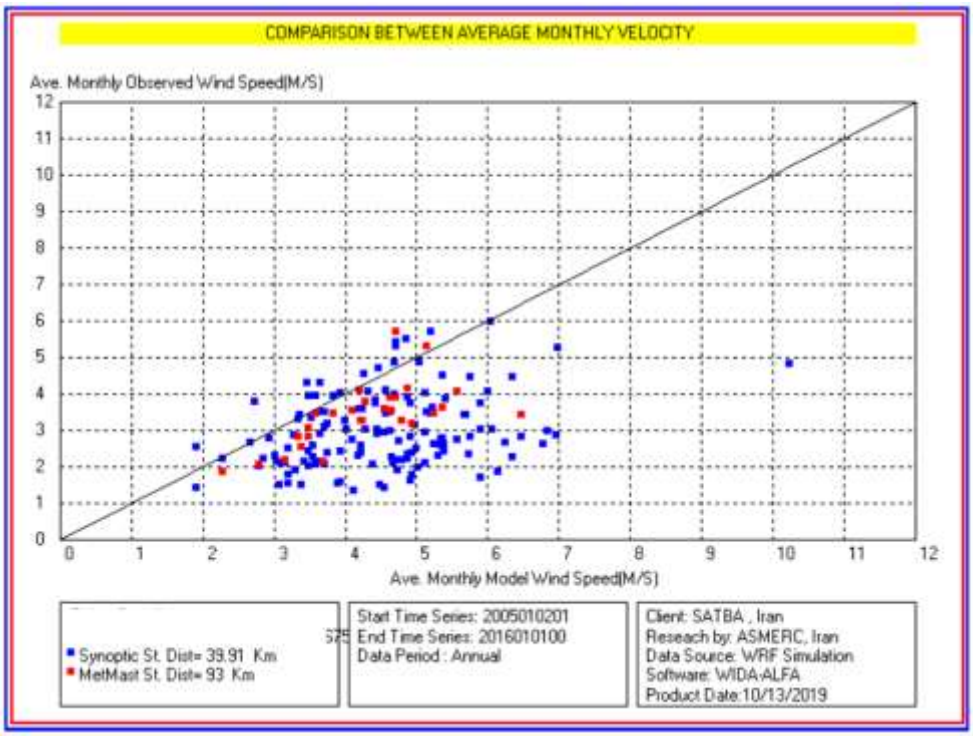

Fig. 20 - Comparison of observed speed with modeled velocity (Region 4)

- **Region 5:** It has a complex topography in the mountainous region, with an altitude of 1000 meters above sea level. The diagrams in this area are shown below.

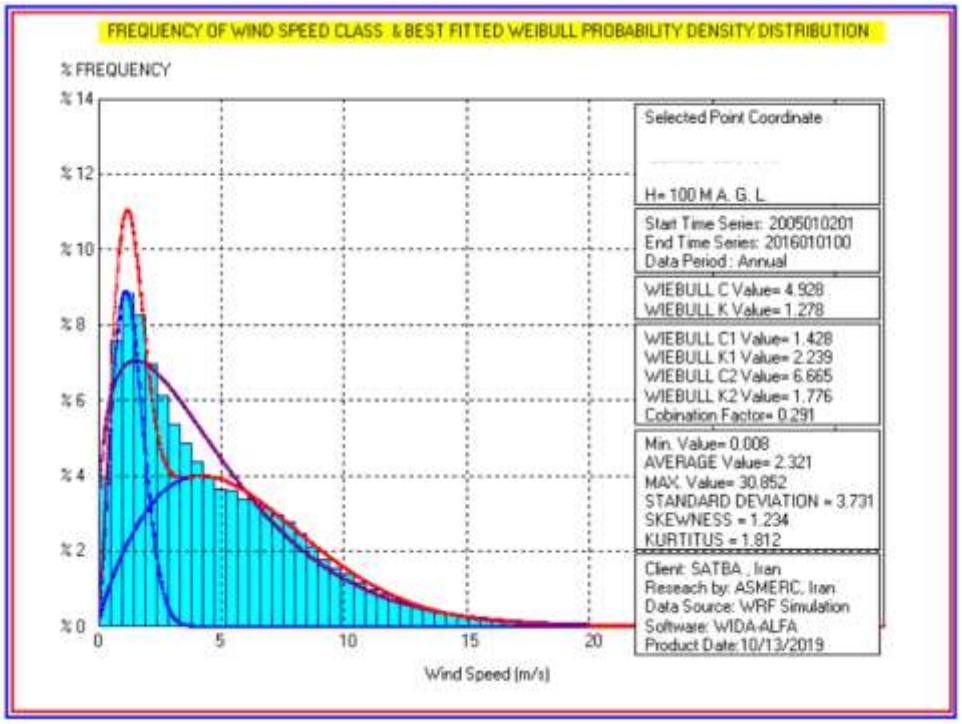

Fig. 21 - Weibul diagram (Region 5)

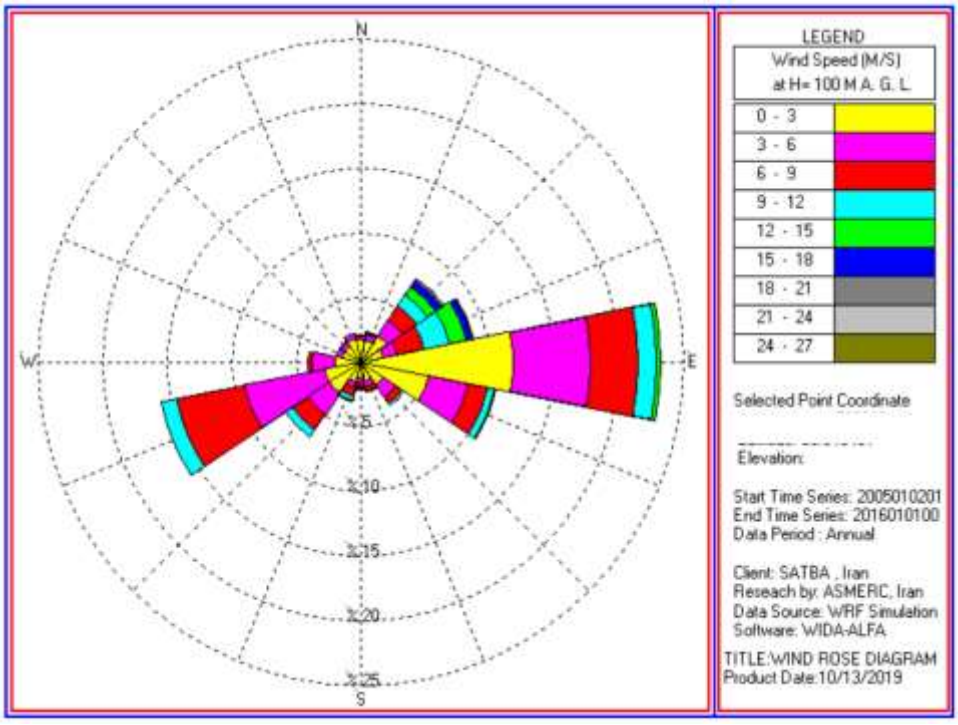

Fig. 22 - Dominant wind direction (Region 5)

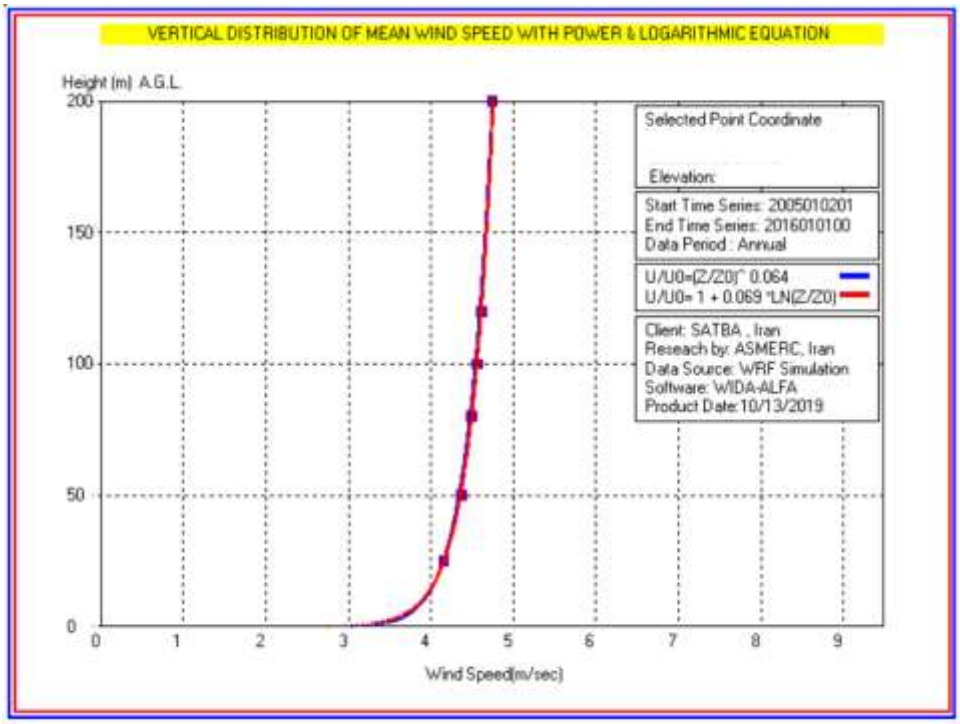

Fig. 23 - Vertical distribution of wind speed with logarithmic equation (Region 5)

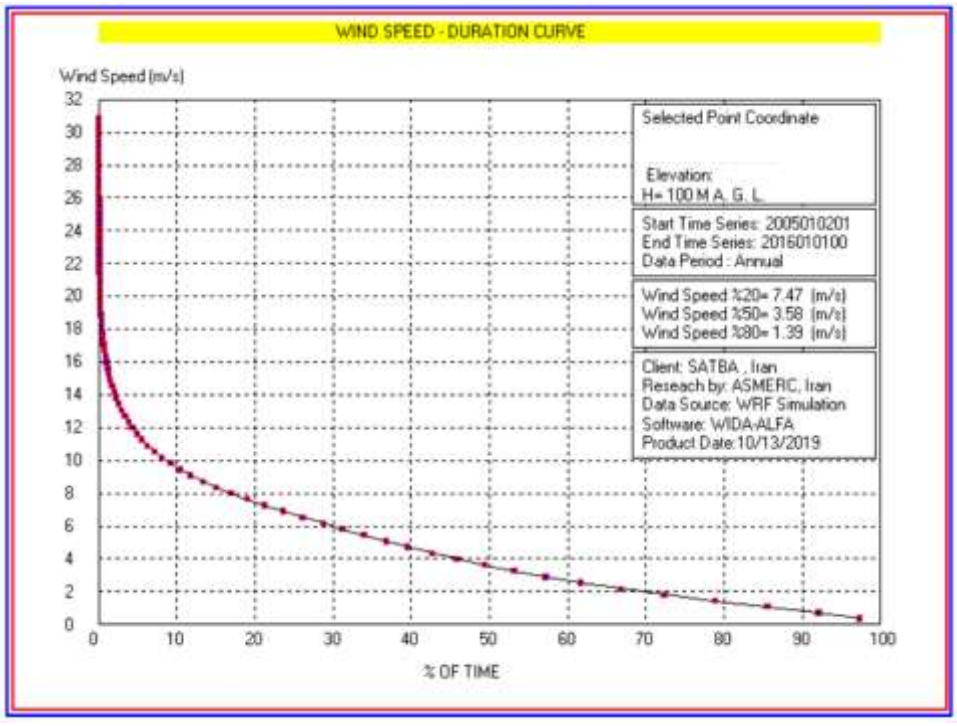

Fig. 24 - Vertical wind speed curve (Region 5)

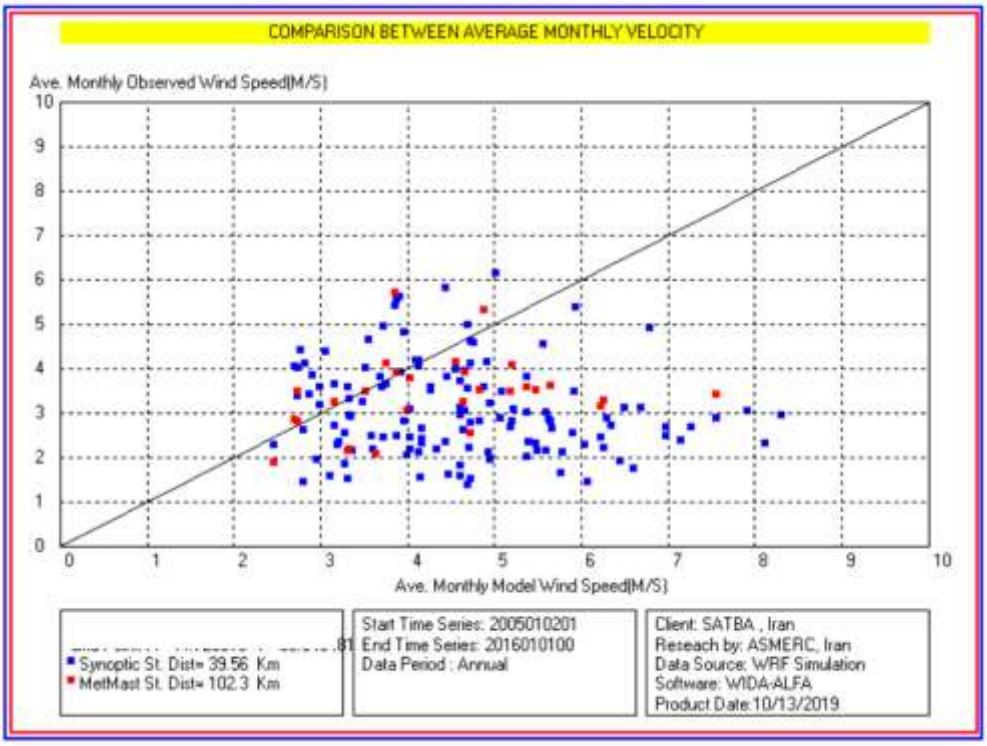

Fig. 25 - Comparison of observed speed with modeled velocity (Region 5)

- **Area 6:** Located in the area of Mahur hill, with a height of 900 meters above sea level. The diagrams in this area are shown below.

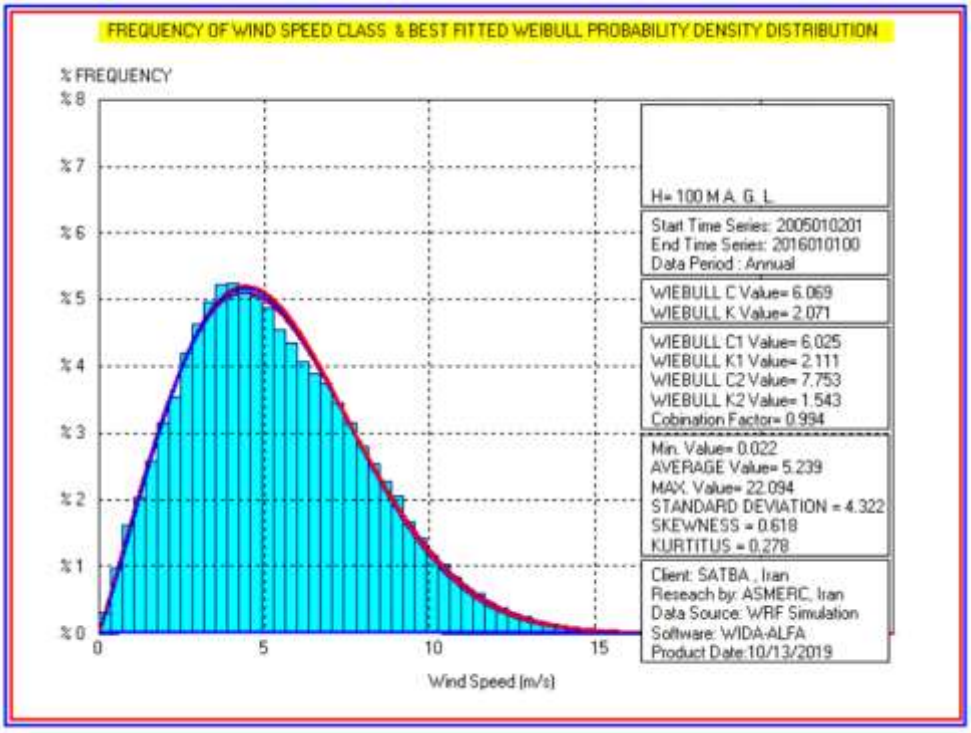

Fig. 26 - Weibul diagram (Region 6)

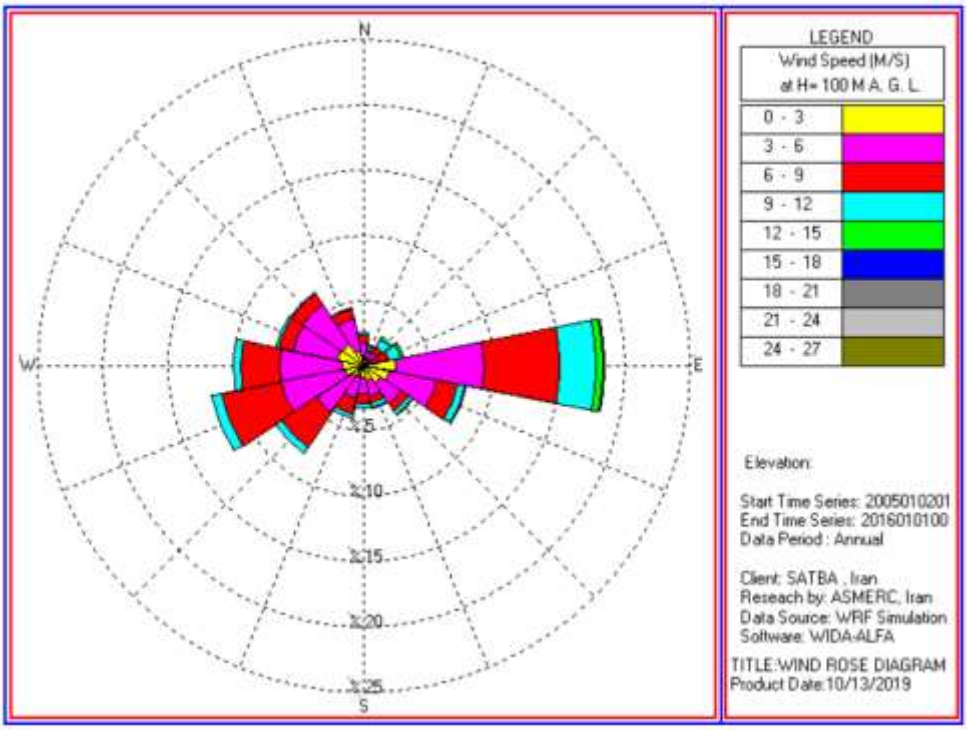

Fig. 27 - Dominant wind direction (Region 6)

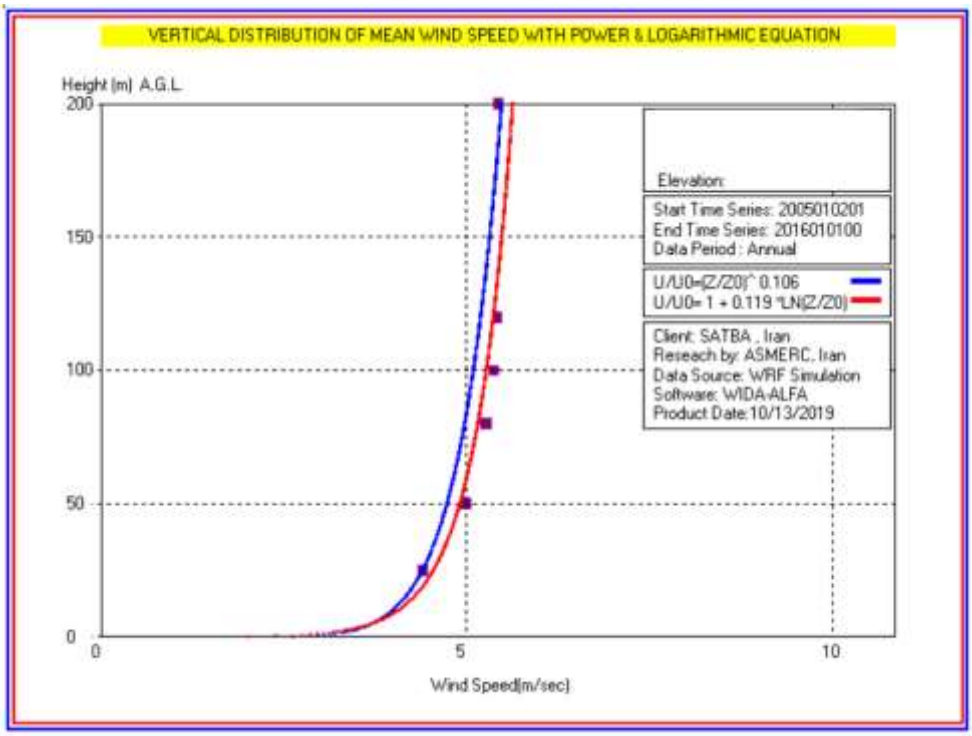

Fig. 28 - Vertical distribution of wind speed with logarithmic equation (Region 6)

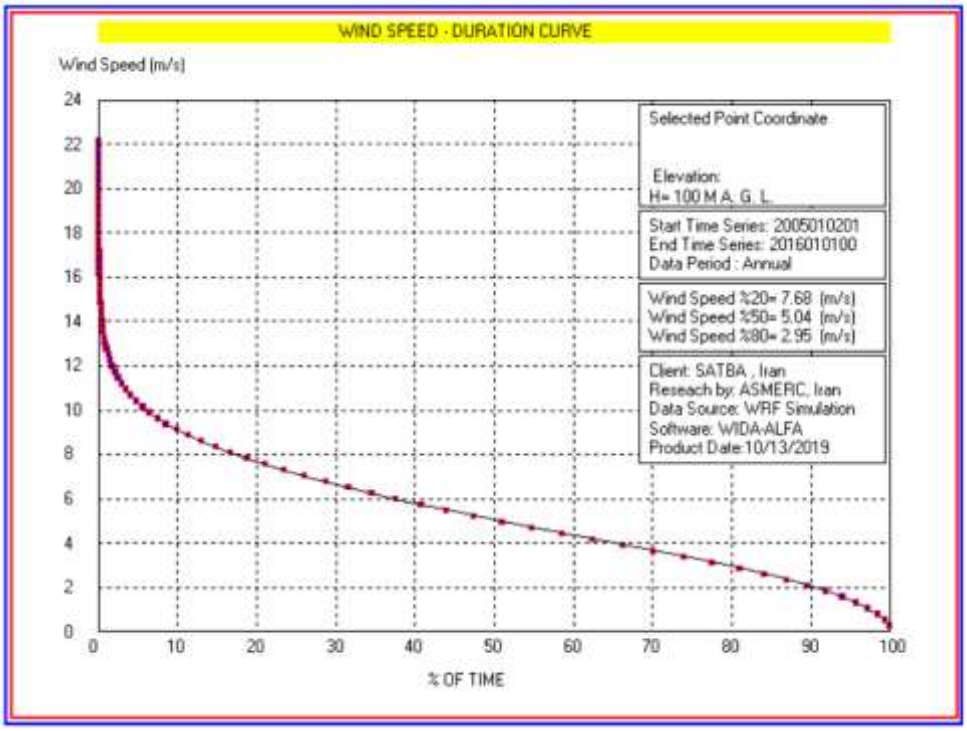

Fig. 29 - Vertical wind speed curve (Region 6)

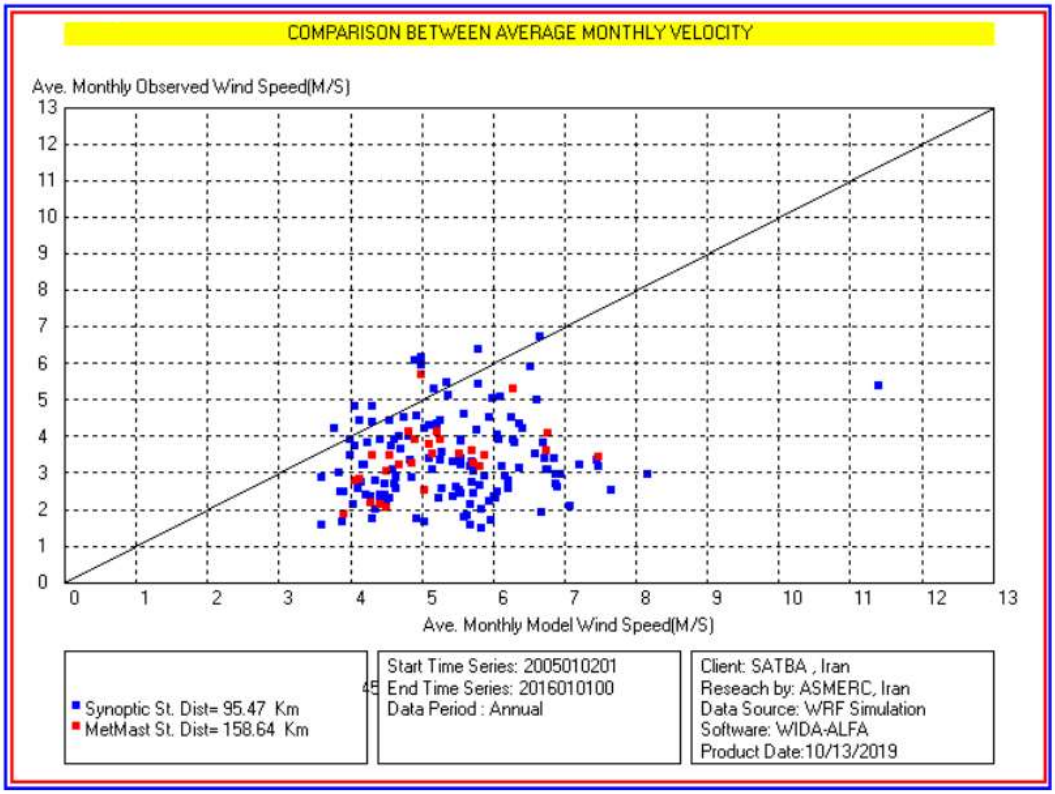

Fig. 30 - Comparison of observed speed with modeled velocity (Region 6)

7. SUMMARY AND CONCLUSION

By modeling the softening of the studied areas, areas with different heights and topographies were evaluated and finally the variables of the wind regime of 6 regions, in Table 2, are compared for comparison as follows.

Table 2 - Models of modeled wind regime of the studied areas

Num	Type of topography of the area	Above sea level (m)	Wind speed (m/s)			Speed at ground level (m/s)	The prevailing wind direction	Ratio speed change to height	Weibull		Standard deviation	Frequency		
			min	Ave	max				c	k		20%	50%	90%
1	Valley - Flat	2200	0.02	5.62	30.5	4	W	0.076	6.67	1.72	4.26	8.62	5.52	2.88
2	Valley - Flat (residential area)	2100	0.01	6.29	30.7	3	E	0.106	5.95	1.2	6.526	9.19	4.25	1.63
3	Flat (residential area)	2000	0.02	6.22	28.9	2	SSW	0.159	6.59	1.44	5.439	9.23	5.16	2.28
4	Mountaintop	2300	0	6.02	33	3.5	SE	0.055	4.92	1.4	3.477	6.96	3.58	1.75
5	Mountainous (Complex topography)	1000	0.01	2.32	30.9	3	E	0.064	4.93	1.28	3.731	7.47	3.58	1.39
6	Rolling Road	900	0.02	5.24	22.1	2.5	E	0.106	6.07	2.07	4.322	7.68	5.04	2.95

In this study, 6 regions have been selected with completely different topographies and different heights by software modeling the wind regime in 6 regions. We have obtained the main variables of the wind regime. The selected points have been selected from the north of the country to the south of the country in the mountainous strip of the northwest of the country, respectively.

According to the above table the following results are obtained:

1- Wind speed on the ground is directly related to the altitude and topography of the region, meaning that the region with higher altitude has higher wind speed and the roughness of the ground plays an important role in shaping the wind regime and the speed of the ground.
2- Wind speed after full formation due to the effect of topography with increasing altitude result in increasing of maximum speed in the region. However, according to the topography of the region and the obtained average speed, the average speed is affected by the topography and has nothing to do with height.
3- The wind direction in these 6 regions according to the modeling, is usually from the east, except two regions from the west. The wind direction in this study is not affected by height and topography and depends on the wind formation in the region.
4- The ratio of speed changes to the height is also directly related to the topography and roughness of the region, the topography of the region is smooth and has minimum roughness. In this study, the minimum of this ratio is 0.55 for mountain peaks and the maximum is 0.159 for residential areas that have artificial barriers in residential areas.
5- In this 6 regions, the hourly changes of average wind speed in comparison to the average annual speed (K), except mahour hill region. Which its value is 2. other region have almost the same value and less than 1.5 , which means that continuity of wind speed in these regions does not have a certain value and the changes in wind speed in one hour have the maximum value and it is not dependent on the topography and height.

6- Finally, according to the variables of Weibull distribution for these regions and the percentage of repetition of the modeled speed for these region, we can see the effect of coefficient (K) on the modeling result. For this purpose In the region of mahour hill , which has k=2 , obtained speeds from modeling are 7.68 , 5.04 and 2.95 which have repetition percentage of 20 , 50 and 90 percent In comparison to other regions which have obvious and acceptable changes . However in other places, this difference between 3 obtained speeds, has more values.

In this study, it is found that codes underestimates topographical effects when terrain is undulating, therefore it requires to investigate more for the terrain of undulating and mountainous. In spite of complexity involved in evaluating the topographical effects for undulating and mountainous terrain, there is an obvious necessity for an international harmonization of calculating methods for the topographical effects, particularly when terrain is undulating.

The proposed method had few limitations such as computational complexity and it depended on the number of iterations, number of universes and universe sorting mechanism. The limitations also included the parameters to be estimated suffered from consistency when the measured wind data was not good. In order to achieve better results the measuring instrument must be properly calibrated before analyzing the data. The proposed MVO technique depended on the geographical location and also on the maximum and minimum wind speed limits. In future work, to forecast the wind speed, the MVO technique should be first implemented to find the Weibull parameters from the wind speed data and create hourly wind speed randomly. Now by applying randomly generated wind data to ANN for matching actual wind speed until the forecasted errors are minimized.

Author Contributions: All authors are involved developing the concept to make the article error free technical outcome for the set investigation work.

REFERENCES

1. Beljaars, A. C. M., A. R. Brown, and N. Wood (2004), A new parametrization of turbulent orographic form drag, Q. J. R. Meteorol. Soc., 130, 1327–1347, doi:10.1256/qj.03.73.
2. Bitsuamlak, G. T., Stathopoulos, T., & Bédard, C. (2004). Numerical evaluation of wind flow over complex terrain. Journal of Aerospace Engineering, 17(4), 135-145.
3. Doms, G., et al. (2011), A description of the nonhydrostatic regional COSMO model, Part II: Physical parameterization, LM F90 4.20 38, Consortium for Small-Scale Modelling, Printed at Deutscher Wetterdienst, Offenbach, Germany.
4. Dutra, E., S. Kotlarski, P. Viterbo, G. Balsamo, P. M. A. Miranda, C. Schär, P. Bissolli, and T. Jonas (2011), Snow cover sensitivity to horizontal resolution, parameterizations, and atmospheric forcing in a land surface model, J. Geophys. Res., 116, D21109, doi: 10.1029/2011JD016061.
5. Fiedler, F., and H. A. Panofsky (1972), The geostrophic drag coefficient and the 'effective' roughness length, Q. J. R. Meteorol. Soc., 98, 213–220.
6. Finardi, S., Morselli, M. G., & Jeannet, P. (1997). Wind flow models over complex terrain for dispersion calculations. In Cost Action (Vol. 710, pp. 12-25).
7. Grant, A. L. M., and P. J. Mason (1990), Observations of boundary-layer structure over complex terrain, Q. J. R. Meteorol. Soc., 116, 159–186.
8. Masson, V., & Bougeault, P. (1996). Numerical simulation of a low-level wind created by complex orography: A Cierzo case study. Monthly weather review, 124(4), 701-715.
9. Mathew, S. (2006). Wind energy: fundamentals, resource analysis and economics (Vol. 1). Heidelberg: Springer.
10. Mueller, K. J., Miller, C., Beatty, K., & Boissonnade, A. (2006, April). Correlation of topographic speed-up factors and building damage ratios for Hurricane Fabian in Burmuda. In Extended abstracts, 27th Conference on Hurricanes and Tropical Meteorology (pp. 24-28).
11. Nedjari, H. D., Guerri, O., & Saighi, M. (2017). CFD wind turbines wake assessment in complex topography. Energy Conversion and Management, 138, 224-236.
12. Pattanapol, W., Wakes, S. J., Hilton, M. J., & Dickinson, K. J. (2011).Effects Of Topography on Wind Flow and Sand Transport & Development Options Ocean Beach Domain.
13. Parajka, J., S. Dadson, T. Lafon, and R. Essery (2010), Evaluation of snow cover and depth simulated by a land surface model using detailed regional snow observations from Austria, J. Geophys. Res., 115, D24117, doi:10.1029/2010JD014086.
14. Peralta, C., Schmidt, J., & Stoevesandt, B. (2014, January). The influence of orographic features on wind farm efficiencies. In ITM Web of Conferences (Vol. 2). EDP Sciences.
15. Jimenez, P. A., and J. Dudhia (2012), Improving the representation of resolved and unresolved topographic effects on surface wind in the WRF model, J. Appl. Meteorol. Climatol., 51, 300–316.
16. Kim, Y. J., S. D. Eckermann, and H. Y. Chun (2003), An overview of the past, present and future of gravity wave drag parametrization for numerical climate and weather prediction models, Atmos. Ocean, 17, 65–98.

17. Leung, L. R., and S. J. Ghan (1995), A subgrid parameterization of orographic precipitation, Theor. Appl. Climatol., 52, 95–118.
18. Mason, P. J. (1985), On the parameterization of the orographic drag, paper persented at Seminar on Physical parametrization for Numerical Models of the Atmosphere, pp. 139–165, ECMWF, Shinfield Park, Reading, Berkshire, U. K.
19. Rontu, L. (2006), A study on parametrization of orography-related momentum fluxes in a synoptic-scale NWP model, Tellus A, 58, 69–81.
20. Rotach, M. W., A. Gohm, M. N. Lang, D. Leukauf, I. Stiperski, and J. S. Wagner (2015), On the vertical exchange of heat, mass, and momentum over complex, mountainous terrain, Front. Earth Sci., 3, 76, doi:10.3389/feart.2015.00076.
21. Ruel, J. C., Pin, D., & Cooper, K. (1998). Effect of topography on wind behaviour in a complex terrain. Forestry: An International Journal of Forest Research, 71(3), 261-265.
22. Rueda, F. J., Schladow, S. G., Monismith, S. G., & Stacey, M. T. (2005). On the effects of topography on wind and the generation of currents in a large multi-basin lake. Hydrobiologia, 532(1), 139-151.
23. Sugimura, T., Takahashi, K., Iida, M., & Center, E. S. (2009). Numerical wind analysis on complex topography using multiscale simulation model. In The seventh International Conference on Urban Climate.
24. Taylor, P. A., R. I. Sykes, and P. J. Mason (1989), On the parameterization of drag over small-scale topography in neutrally-stratified boundary-layer flow, Boundary Layer Meteorol., 48, 409–422.
25. Wood, N., and P. Mason (1993), The pressure force induced by neutral, turbulent flow over hills, Q. J. R. Meteorol. Soc., 119(514), 1233–1267.
26. Wood, N., A. R. Brown, and F. E. Hewer (2001), Parametrizing the effects of orography on the boundary layer: An alternative to effective roughness lengths, Q. J. R. Meteorol. Soc., 127, 759–777.

27. Ouarda, T.B.M.J.; Charron, C.; Chebana, F. Review of criteria for the selection of probability distributions for wind speed data and introduction of the moment and L-moment ratio diagram methods, with a case study. Energy Convers. Manag. 2016, 124, 247–265.
28. Jaramillo, O.A.; Borja, M.A. Wind speed analysis in La Ventosa, Mexico: A bimodal probability distribution case. Renew. Energy 2004, 29, 1613–1630.
29. Wang, B.; Cot, L.D.; Adolphe, L.; Geffroy, S. Estimation of wind energy of a building with canopy roof. Sustain. Cities Soc. 2017, 35, 402–416.
30. Pishgar-Komleh, S.H.; Keyhani, A.; Sefeedpari, P. Wind speed and power density analysis based on Weibull and Rayleigh distributions (a case study: Firouzkooh county of Iran). Renew. Sustain. Energy Rev. 2015, 42,313–322.
31. Maatallah, T.; El Alimi, S.; Wajdi Dahmouni, A.; Nasrallah, S.B. Wind power assessment and evaluation of electricity generation in the Gulf of Tunis, Tunisia. Sustain. Cities Soc. 2013, 6, 1–10.